Subsurface Imaging 3-D Objects in Multilayered Media by Using Electromagnetic Inverse Scattering Series Method (EISSM)

J. G. Wang[1], Z. Q. Zhao[1], Z. P. Nie[1], and Q. H. Liu[2]

[1]School of Electronic Engineering
University of Electronic Science and Technology of China, China
[2]Department of Electrical and Computer Engineering, Duke University, USA

Abstract— Subsurface imaging 3-D objects buried in layered medium with electromagnetic waves has recently attracted significant interests. Due to the uncertainty of dielectric parameters of layered background media in practice, most of existing electromagnetic inverse methods reconstruct the buried objects unfaithfully. In order to accurately reconstruct the objects buried in multilayered media with unknown dielectric parameters, we develop a new imaging method named electromagnetic inverse scattering series method (EISSM) for imaging 3-D objects in multilayered media. The 3-D EISSM combines the inverse scattering series (ISS) theory with a multi-array tomographic approach. It directly reconstructs the positions of the buried objects (not their dielectric properties) solely with the dielectric parameters of free space according to the discontinuities of dielectric parameters. Moreover, the effects of multilayered media to the position error predicted by EISSM are also analyzed and discussed. Aiming to validate the feasibility of the developed 3-D EISSM, some numerical simulations are given as well as the results reconstructed by commonly used time reversal mirror (TRM) technique. Through the simulations, the EISSM is capable of positioning 3-D targets buried in multilayered media with less error than traditional TRM.

1. INTRODUCTION

Subsurface imaging 3-D objects buried in multilayered media with electromagnetic waves has recently attracted significant attentions and been extensively studied. Up to now, various algorithms have been proposed to circumvent the inherent difficulties in different application backgrounds [1–5]. However, most of existing electromagnetic inverse methods are based on the assumptions that the dielectric parameters of multilayered media are exactly known. Owing to the uncertainty of dielectric parameters of the layered background media in practice, existing methods in [1–5] will reconstruct the buried objects unfaithfully.

Aiming to accurately reconstruct the buried objects in practice conditions (the dielectric parameters of multilayered media are unknown), a modified inverse scattering series method (MISS) based on the inverse scattering series (ISS) theory was developed in hydrocarbon exploration for 1-D and 2-D scenarios [6]. The MISS method reconstructs the electric conductivity of objects with an approximation that the dielectric permittivity is constant and equal to the value of water.

Different to the MISS method, we develop an imaging method named electromagnetic inverse scattering series method (EISSM) for imaging 3-D objects buried in multilayered media. The proposed EISSM combines the ISS idea with a multi-array tomographic approach [7]. It directly reconstructs the positions of the buried objects (not their dielectric properties) solely with the dielectric parameters of free space according to the discontinuities of dielectric parameters. Moreover, the effects of multilayered media to the position error predicted by EISSM are also analyzed and discussed. In order to validate the feasibility of the developed EISSM, some numerical simulations are given as well as the results reconstructed by commonly used time reversal mirror (TRM) technique [8, 9]. Through the simulations, the EISSM is capable of positioning 3-D targets buried in multilayered media with less error than traditional TRM.

2. THEORY

Figure 1 shows the configuration of a 3-D object buried in a layered medium. In order to avoid the mutual coupling, an antenna array which consists of a sequence of monostatic pairs is applied. When a given transmitter emits an electromagnetic pulse, only the corresponding receiver is activated [7]. In addition, the transmitters are assumed as z-directed electric dipoles.

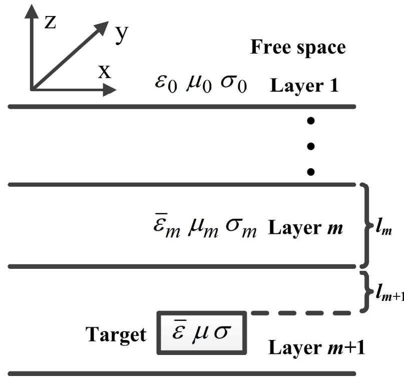

Figure 1: Typical configuration of an object in a layered medium.

For the model in Figure 1, the wave equations for electric field in the actual medium and free space are expressed as

$$\left(\nabla^2 + k_m^2\right)\mathbf{E}(\mathbf{r}, \mathbf{r}_s) = -\mathbf{J}(\omega)\delta(\mathbf{r} - \mathbf{r}_s), \tag{1}$$

$$\left(\nabla^2 + k_0^2\right)\mathbf{E}_0(\mathbf{r}, \mathbf{r}_s) = -\mathbf{J}(\omega)\delta(\mathbf{r} - \mathbf{r}_s), \tag{2}$$

where $k_m = \omega\sqrt{\bar{\varepsilon}_m\mu_m}$, $k_0 = \omega\sqrt{\varepsilon_0\mu_0}$, ($\bar{\varepsilon}_m$, σ_m, μ_m) are the permittivity, conductivity and permeability of the actual layered medium m, ($\bar{\varepsilon}$, σ, μ) are the permittivity, conductivity and permeability of the target, (ε_0, σ_0, μ_0) are the permittivity, conductivity and permeability of free space. $\mathbf{J}$ is an excitation source, ω is the angular frequency, the field point $\mathbf{r} = (x, y, z)$ and the position of source $\mathbf{r}_s = (x_s, y_s, z_s)$.

Define a perturbation operator as

$$\beta = \left(\nabla^2 + k_m^2\right) - \left(\nabla^2 + k_0^2\right) = \omega^2\varepsilon_0\mu_0\left[(\bar{\varepsilon}_m\mu_m/\varepsilon_0\mu_0) - 1\right] = k_0^2\alpha, \tag{3}$$

where the dielectric perturbation $\alpha = (\bar{\varepsilon}_m\mu_m/\varepsilon_0\mu_0) - 1$. In this paper, μ_m and μ are assumed as μ_0.

According to the Lippmann-Schwinger equation, electric field $\mathbf{E}$ is rewritten as

$$\mathbf{E}(\mathbf{r}, \mathbf{r}_s) = \mathbf{E}_0(\mathbf{r}, \mathbf{r}_s) + \int_D G_0(\mathbf{r}, \mathbf{r}')\beta(\mathbf{r}')\mathbf{E}(\mathbf{r}', \mathbf{r_s})d\mathbf{r}', \tag{4}$$

where G_0 is the Green's function of free space, D is the image domain.

Assume $\mathbf{E} = \mathbf{E}_0 + \mathbf{E}_1 + \ldots + \mathbf{E}_n + \ldots = \sum_{n=0}^{+\infty}\mathbf{E}_n$, substitute it into (4) and therefore (4) can be successively iterated for field $\mathbf{E}$ on the right hand side,

$$\mathbf{E}_1(\mathbf{r}, \mathbf{r}_s) = \int_D G_0(\mathbf{r}, \mathbf{r}')\beta(\mathbf{r}')\mathbf{E}_0(\mathbf{r}', \mathbf{r}_s)d\mathbf{r}' \overset{Denote}{\Rightarrow} (G_0\beta\mathbf{E}_0), \tag{5}$$

$$\mathbf{E}_2(\mathbf{r}, \mathbf{r}_s) = \int_D G_0(\mathbf{r}, \mathbf{r}')\beta(\mathbf{r}')\mathbf{E}_1(\mathbf{r}', \mathbf{r}_s)d\mathbf{r}' \overset{Denote}{\Rightarrow} (G_0\beta\mathbf{E}_1), \tag{6}$$

$$\ldots$$

$$\mathbf{E}_n(\mathbf{r}, \mathbf{r}_s) = \int_D G_0(\mathbf{r}, \mathbf{r}')\beta\left(\mathbf{r}'\right)\mathbf{E}_{n-1}\left(\mathbf{r}', \mathbf{r}_s\right)d\mathbf{r}' \overset{Denote}{\Rightarrow} (G_0\beta\mathbf{E}_{n-1}), \quad n = 1, 2, \ldots, +\infty. \tag{7}$$

Then the scattered field is

$$\begin{aligned}\mathbf{E_s} &= \mathbf{E} - \mathbf{E}_0 = \mathbf{E}_1 + \mathbf{E}_2 + \mathbf{E}_3 + \ldots = (G_0\beta\mathbf{E}_0) + (G_0\beta\mathbf{E}_1) + (G_0\beta\mathbf{E}_2) + \ldots \\ &= (G_0\beta\mathbf{E}_0) + (G_0\beta(G_0\beta\mathbf{E}_0)) + (G_0\beta[G_0\beta(G_0\beta\mathbf{E}_0)]) + \ldots.\end{aligned} \tag{8}$$

Assume β and α as a sum of constituent terms,

$$\beta = \beta_1 + \beta_2 + \ldots + \beta_n + \ldots = \sum_{n=1}^{+\infty}\beta_n = k_0^2\alpha = k_0^2\alpha_1 + k_0^2\alpha_2 + \ldots + k_0^2\alpha_n + \ldots = k_0^2\sum_{n=1}^{+\infty}\alpha_n, \tag{9}$$

where β_n and α_n are the nth part of β and α, respectively.

Substitute (9) into (8)

$$\begin{aligned}\mathbf{E_s}(\mathbf{r_M},\mathbf{r}_s) &= \left(G_0\left(\sum_{n=1}^{+\infty}\beta_n\right)\mathbf{E}_0\right)+\left(G_0\left(\sum_{n=1}^{+\infty}\beta_n\right)\left(G_0\left(\sum_{n=1}^{+\infty}\beta_n\right)\mathbf{E}_0\right)\right)+\ldots\\ &= (G_0\beta_1\mathbf{E}_0)+(G_0\beta_2\mathbf{E}_0)+(G_0\beta_3\mathbf{E}_0)+\ldots+(G_0\beta_1(G_0\beta_1\mathbf{E}_0))+(G_0\beta_1(G_0\beta_2\mathbf{E}_0))\\ &\quad+(G_0\beta_2(G_0\beta_1\mathbf{E}_0))+\ldots+(G_0\beta_1(G_0\beta_1(G_0\beta_1\mathbf{E}_0)))+\ldots, \end{aligned} \tag{10}$$

where $\mathbf{E}_s(\mathbf{r_M},\mathbf{r}_s)$ is the scattered field measured at the positions of receivers $\mathbf{r}_M$.

Match the equal order of β_n and therefore the solution of (10) is equivalent to solve following equations

$$\left(G_0k_0^2\alpha_1\mathbf{E}_0\right)=\mathbf{E_s}(\mathbf{r_M},\mathbf{r_s}), \tag{11}$$

$$\left(G_0k_0^2\alpha_2\mathbf{E}_0\right)+\left(G_0k_0^2\alpha_1\left(G_0k_0^2\alpha_1\mathbf{E}_0\right)\right)=0, \tag{12}$$

$$\begin{aligned}&\left(G_0k_0^2\alpha_3\mathbf{E}_0\right)+\left(G_0k_0^2\alpha_1\left(G_0k_0^2\alpha_2\mathbf{E}_0\right)\right)+\left(G_0k_0^2\alpha_2\left(G_0k_0^2\alpha_1\mathbf{E}_0\right)\right)\\ &+\left(G_0k_0^2\alpha_1\left(G_0k_0^2\alpha_1\left(G_0k_0^2\alpha_1\mathbf{E}_0\right)\right)\right)=0,\end{aligned} \tag{13}$$

$$\ldots$$

By using Fourier transform and inverse Fourier transform, one can solve (11) with (3) for α_1,

$$\alpha_1(x,y,z)=-8\frac{\cos^3\theta_0}{c_0}\mathrm{Ez}_s\left(\mathbf{r_M},\mathbf{r_s};\frac{\cos\theta_0}{c_0}(2z-z_m-z_s)+\frac{\sin\theta_0}{c_0}\right), \tag{14}$$

where θ_0 is the incident angle, $x=(x_m+x_s)/2$, $y=(y_m+y_s)/2$, $\mathbf{r_M}=(x_m,y_m,z_m)$, $\mathbf{r_s}=(x_s,y_s,z_s)$. $\mathrm{Ez}_s(\mathbf{r_M},\mathbf{r_s};t)$ is the z-directed electric field data measured by the receiver at position $\mathbf{r_M}$.

Then substitute α_1 into (12) to solve for α_2, and so on. Finally, α is constructed by summing a series of constituent terms, i.e.,

$$\alpha(x,y,z)=\sum\nolimits_{n=1}^{\infty}\frac{(-1/2)^{n-1}}{(n-1)!\cos^{2(n-1)}\theta_0}\cdot\left[\int_{z_s}^{z}\alpha_1(x,y,z')dz'\right]^{n-1}\cdot\frac{\partial^{n-1}\alpha_1(x,y,z)}{\partial z^{n-1}}. \tag{15}$$

By using the differential properties of Fourier transform over α_1, a closed form of α is derived as

$$\alpha_{\mathrm{EISSM}}(x,y,z)=\alpha_1(x,y,z-\Delta), \tag{16}$$

where $\Delta=(2\cos^2\theta_0)^{-1}\int_{z_s}^{z}\alpha_1(x,y,z')dz'$. Detailed derivation can be referred to [10].

In (16), α_{EISSM} is an approximate solution of actual α in (15) because it encapsulates an infinite number of terms through a manipulation of the depth variable z in α_1. So, an error will be produced by using EISSM for positioning the buried target.

In order to well understand the error of EISSM, the position error predicted by α_1 is firstly discussed. For simplicity, the transmitters and receivers are assumed to be placed on the same plane ($z_s=z_m$). So the position predicted by α_1 is

$$\hat{z}_R\ =\int_{z_s}^{z_R}\frac{\cos\theta_0}{c_0/\sqrt{\varepsilon_r(x,y,z')}}dz'\times\frac{c_0}{\cos\theta_0}+z_s=\int_{z_s}^{z_R}\sqrt{\varepsilon_r(x,y,z')}dz'+z_s, \tag{17}$$

where z_R is the real position of target. According to (14), α_1 uses c_0 of free space to position the target buried in the layered medium. The position error of α_1 is

$$\Delta\delta_{\alpha_1}\ =\hat{z}_R-z_R=\int_{z_s}^{z_R}\sqrt{\varepsilon_r(x,y,z')}dz'+z_s-z_R=\int_{z_s}^{z_R}(\sqrt{\varepsilon_r(x,y,z')}-1)dz'. \tag{18}$$

From (16), the position reconstructed by EISSM is $\hat{z}_{\mathrm{EISSM}}=\hat{z}_R+\Delta$. Then the error in position predicted by EISSM is

$$\begin{aligned}\Delta\delta_{\mathrm{EISSM}}&=\hat{z}_{\mathrm{EISSM}}-z_R=\underbrace{\hat{z}_R-z_R}_{\Delta\delta_{\alpha_1}}+\Delta=\int_{z_s}^{z_R}\left(\sqrt{\varepsilon_r(x,y,z')}-1\right)dz'+\frac{\int_{z_s}^{z_R}\alpha_1(x,y,z')dz'}{2\cos^2\theta_0}\\ &=\int_{z_s}^{z_R}\left(\sqrt{\varepsilon_r(x,y,z')}-1\right)dz'-\frac{4\cos\theta_0}{c_0}\int_{z_s}^{z_R}\mathrm{Ez}_s\left(\mathbf{r_M},\mathbf{r_s};\frac{\cos\theta_0}{c_0}(2z'-z_m-z_s)+\frac{\sin\theta_0}{c_0}\right)dz'.\end{aligned} \tag{19}$$

For the planar layered medium shown in Figure 1, (19) can be rewritten as

$$\Delta\delta_{\mathrm{EISSM}} = \sum_{i=2}^{m+1}(\sqrt{\varepsilon_r(i)}-1)l_i - \frac{4\cos\theta_0}{c_0}\int_{z_s}^{z_R} \mathrm{Ez}_s(\mathbf{r_M},\mathbf{r_s};\frac{\cos\theta_0}{c_0}(2z'-z_m-z_s)+\frac{\sin\theta_0}{c_0})dz', \quad (20)$$

where $\varepsilon_r(i)$ is the relative permittivity of layered medium i and assumed as a constant in layered medium i ($i = 2, 3, \ldots, m+1$). l_i is the z-direction thickness of layered medium i ($i = 2, 3, \ldots, m$), l_{m+1} is the depth that the target embedded in layered medium $m + 1$, and $\sum_{i=2}^{m+1} l_i = z_R$.

In (20), the incident angle θ_0 and the measured data Ez_s are fixed when the transmitters and receivers are given. So $\Delta\delta_{\mathrm{EISSM}}$ relates with z_R, $\varepsilon_r(i)$ and l_i of layered medium according to (20).

3. NUMERICAL SIMULATIONS

In order to demonstrate the feasibility of the proposed method, Figure 2 shows a scenario of a 3-D target buried in the bottom of a three-layer medium. 18 z-directed electric dipole antennas are co-located to form 9 monostatic pairs with a uniformly space of 15 cm. When a given dipole transmitter emits a pulse, only the corresponding receiver is activated [7]. 9 transmitters operate sequentially until completing one full cycle of activations. Then the antenna array moves along $+x$ direction (scan line) for surveying. In the simulations, the antenna array moves 9 times evenly along $+x$ direction with an interval of 15 cm. A pulse of Blackman-Harris window (BHW) function with characteristic frequency of 1.5 GHz is used as a source signal. The dielectric constant and conductivity of the three layers and the target are $(\varepsilon_r, \sigma) = (1.0, 0.0\,\mathrm{S/m})$, (2.0, 0.01 S/m), (3.4, 0.01 S/m) and (9.0, 2.0 S/m), respectively. The size of the target is 20 cm × 20 cm × 5 cm. The synthesis data are generated by using FDTD method.

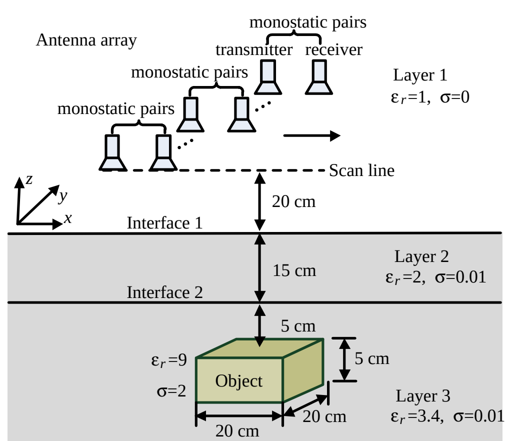

Figure 2: Configuration of an object in a three-layer medium.

With the synthesis data, the results reconstructed under different conditions are given in Figure 3. In practice conditions, the dielectric parameters of layered background medium are unknown. So, Figure 3(a) shows the result reconstructed by using time reversal mirror (TRM) technique solely with the dielectric parameters of free space. Here, Figure 3(a) is used as a reference because TRM has been widely used for surface-penetrating radar detection [8]. In Figure 3(a), the interface 1 is accurately reconstructed because the layer 1 is just free space, while the interface 2 is difficult to detect. The target reconstructed by TRM shifts about 12.9 cm downward to the actual one with the dielectric parameters of free space. Figure 3(b) gives the result reconstructed by using the EISSM under the same conditions as Figure 3(a). The interface 1 is accurately imaged and the interface 2 has a 3.6 cm error downward to the actual one. The buried target reconstructed by the EISSM deviates about 6.0 cm downward to the actual one. Compared with the TRM, the EISSM positions the buried target with more accuracy. To simulate more realistic scenario, Gaussian noise is added to the measured data. The result reconstructed by the EISSM at an SNR of 5 dB is given in Figure 3(c). From Figure 3(c), Gaussian noise does not affect the positions of subsurface scatters predicted by the EISSM and just decrease the image contrast.

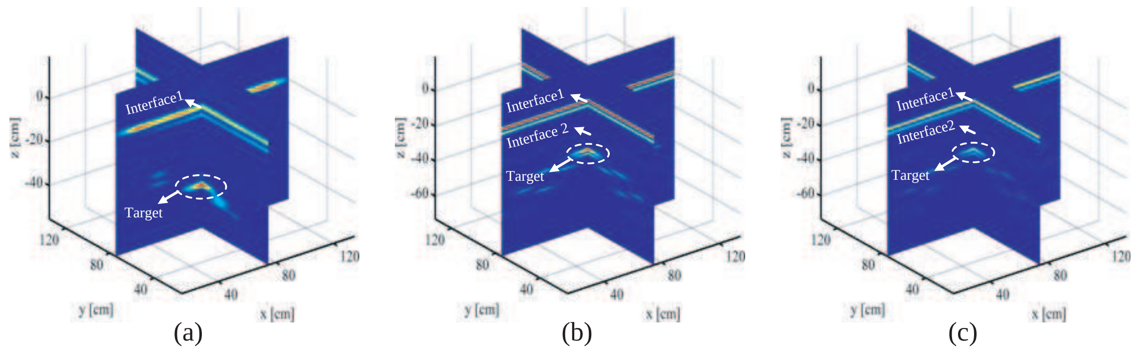

Figure 3: Results reconstructed by using (a) TRM with the dielectric parameters of free space; (b) EISSM with the dielectric parameters of free space; (c) EISSM with the dielectric parameters of free space at SNR = 5 dB.

4. CONCLUSION

This paper presents an electromagnetic inverse scattering series method (EISSM) for sensing 3-D object buried in planar multilayered media with unknown dielectric parameters. The advantage of the EISSM is that it can locate the concealed target without knowing the exact dielectric parameters of multilayered media. Numerical results demonstrate that the EISSM can position the target buried in multilayered media with more accuracy than traditional TRM by solely using the dielectric parameters of free space. For the measured data with Gaussian noise, the EISSM still obtain good results. The developed EISSM is potentially useful for subsurface sensing the concealed targets in practice conditions.

REFERENCES

1. Li, F., Q. H. Liu, and L.-P. Song, "Three-dimensional reconstruction of objects buried in layered media using Born and distorted Born iterative methods," *IEEE Geosci. Remote. Sens. Lett.*, Vol. 1, No. 2, 107–111, 2004.
2. Song, L. P., Q. H. Liu, F. Li, and Z. Q. Zhang, "Reconstruction of three-dimensional objects in layered media: Numerical experiments," *IEEE Trans. Antennas Propag.*, Vol. 53, No. 4, 1556–1561, 2005.
3. Yu, C., M. Yuan, Y. Zhang, J. Stang, R. T. George, G. A. Ybarra, W. T. Joines, and Q. H. Liu, "Microwave imaging in layered media: 3-D image reconstruction from experimental data," *IEEE Trans. Antennas Propag.*, Vol. 58, No. 2, 440–448, 2010.
4. Yu, C., M. Yuan, and Q. H. Liu, "Reconstruction of 3D objects from multi-frequency experimental data with a fast DBIM-BCGS method," *Inv. Probl.*, Vol. 25, No. 2, 024007, 2009.
5. Wei, B., E. Simsek, C. Yu, and Q. H. Liu, "Three dimensional electromagnetic nonlinear inversion in layered media by a hybrid diagonal tensor approximation stabilized biconjugate gradient fast Fourier transform method," *Waves Random Complex Media*, Vol. 17, No. 1, 129–147, Feb. 2007.
6. Kwon, M. J., "Two unconventional approaches to electromagnetic inversion-hierarchical Bayesian inversion and inverse scattering series," Master Thesis, Colorado School of Mines, 2013.
7. Soldovieri, F., G. Prisco, and R. Solimene, "A multiarray tomographic approach for trough-wall imaging," *IEEE Trans. Geosci. Remote Sens.*, Vol. 46, No. 4, 1192–1199, 2008.
8. Cresp, A., I. Aliferis, M. J. Yedlin, C. Pichot, and J. Y. Dauvignac, "Investigation of time-reversal processing for surface-penetrating radar detection in a multiple-target configuration," *Proc. 5th European Radar Conference*, 144–147, Amsterdam, Netherlands, Oct. 30–31, 2008.
9. Cresp, A. and M. J. Yedlin, "Comparison of the time-reversal and SEABED imaging algorithms applied on ultra-wideband experimental SPR data," *Proc. 7th European Radar Conference*, 360–363, 2010.
10. Shaw, S. A., "An inverse scattering series algorithm for depth imaging of reflection data from a layered acoustic medium with an unknown velocity model," Dissertation, 2005.